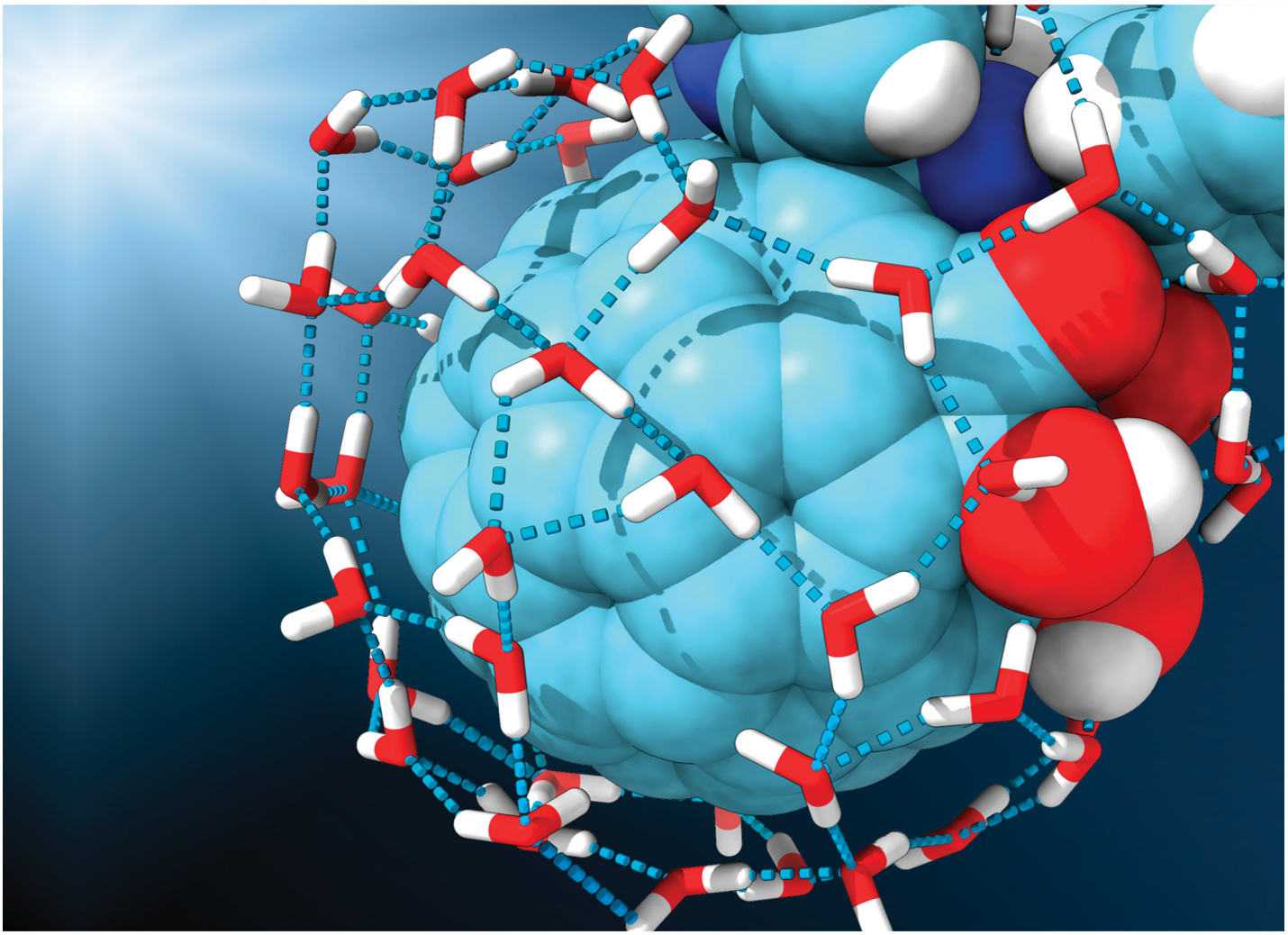

Showcasing research from Professor Yasujiro Murata's laboratory, Institute for Chemical Research, Kyoto University, Kyoto, Japan.

Open-[60]fullerenols with water adsorbed both inside and outside

Water's adsorptive ability toward the external sphere of an open-[60]fullerenol was found to be considerably altered by internal single-water adsorption within the [60]fullerene cavity. Reflecting the electron deficiency of [60]fullerenols, aggregated water became acidic as confirmed by synchrotron IR spectroscopically.

As featured in:

See Yoshifumi Hashikawa, Yasujiro Murata *et al.*, *Chem. Commun.*, 2024, **60**, 1261.

ROYAL SOCIETY OF CHEMISTRY

rsc.li/chemcomm

Registered charity number: 207890

ChemComm

COMMUNICATION

View Article Online
View Journal | View Issue

Cite this: *Chem. Commun.*, 2024, **60**, 1261

Received 10th November 2023,
Accepted 19th December 2023

DOI: 10.1039/d3cc05542f

rsc.li/chemcomm

Open-[60]fullerenols with water adsorbed both inside and outside†

Yoshifumi Hashikawa, *[a] Shumpei Sadai,[a] Yuka Ikemoto [b] and Yasujiro Murata *[a]

The water affinity on [60]fullerenols was found to be governed by surface electrostatic potential while water aggregation is initiated by the hydroxy groups attached on the carbon surface. The molecular water adsorption at the internal sphere caused a significnat inhibition of water adsorption at the external carbon surface.

Water confined between graphene layers is known to adopt a regular ordering on the two-dimensional surface, thus exhibiting a characteristic chemical/physical feature that is otherwise invisible in a bulk environment.[1] Likewise, water inside carbon nanotubes[2] or fullerenes[3] has attracted considerable attention owing to its unique dimensionalities which are offered by the internal curved π-surface of carbon nanomaterials. In contrast, a lack of experimental studies has hampered understanding in depth the interactions and structures of water aggregated on the external π-surface of fullerenes. This is because of very low solubility in an aqueous medium ($<10^{-9}$ mg L^{-1}) as well as a high degree of aggregation.[4] Nevertheless, computational investigations have predicted stable wetting processes of fullerenes.[5]

Polydisperse aqueous systems of [60]fullerene, which are colloids rather than true solutions, could be prepared experimentally wherein [60]fullerene aggregates generate fractal clusters with a diameter range of one to several tens of nanometres.[6] According to molecular dynamics simulations, water–[60]fullerene interactions are governed by relatively strong dispersive van der Waals attraction[7] while hydrogen-bonding (H-bonding) networks contain a mixture of quasi-pentagonal/hexagonal forms with multiple defects induced by dangling hydroxy groups.[8] Bovine serum albumin is a biocompatible solubilizer for [60]fullerene in aqueous media, in which unfolding of the albumin exposes its inner hydrophobic residues which enhance interactions with [60]fullerene.[9] Even in the albumin, [60]fullerene still maintains its cytotoxicity, implying its potential for biological applications. The introduction of multiple functional groups having high affinity to water is a popular approach to access synthetic water-soluble [60]fullerenes and/or [60]fullerenols.[10] At a water–solvent phase boundary, they could arrange in a two-dimensional sheet with a precise thickness at an order of nanometres.[11] Furthermore, stable exfoliation of graphene could be achieved by reactions with [60]fullerenols in a water phase since intercalated [60]fullerenols inhibit the restacking of the graphene sheets.[12] Thus, it is of particular importance to clarify the adsorptive behaviour/structure of water on the [60]fullerene surface (Fig. 1) for the advanced design of [60]fullerenols for their biological and materials science applications. However, controlled hydroxylation of [60]fullerene is, in general, not feasible, thus producing an isomeric mixture which possesses 15 to 18 hydroxy groups with different dispositions.[13] Then, a clear picture on the surface adsorption behaviour of water onto [60]fullerenols is hard to be obtained using an experimental approach so that a computational approach has long been employed, which is

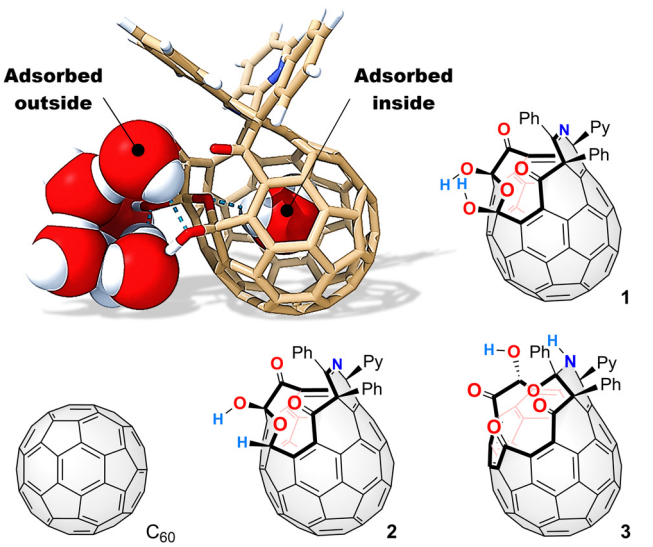

Fig. 1 Adsorption model and structures of open-[60]fullerenols studied herein.

[a] *Institute for Chemical Research, Kyoto University, Uji, Kyoto 611-0011, Japan*
[b] *Japan Synchrotron Radiation Research Institute, Sayo-gun, Hyogo 679-5198, Japan*

† Electronic supplementary information (ESI) available: Optimized geometries. See DOI: https://doi.org/10.1039/d3cc05542f

the only viable solution to this problem.[14] Herein, we studied the adsorption behaviour of water onto three open-[60]fullerenols as well as pristine [60]fullerene using IR microspectroscopy at variable humidity (VH) (Fig. 1). We also disclosed a significant depletion of external water adsorbed on the open-[60]fullerenol surface, being perturbed by internal water trapped within the [60]fullerene cavity.

To verify the water adsorptive behaviour on the surface of a powdery [60]fullerene sample, we performed synchrotron IR microspectroscopy[15] at 300 K with different relative humidities (RHs). As a result, two sharp bands were observed at ν 1427 and 1180 cm^{-1} (Fig. S1a, ESI†), which corresponded to cage vibrations of [60]fullerene, whereas any band related to aggregated water could not be detected so that differential spectra are featureless even at RH = 87% (Fig. S1b, ESI†), implying negligible water adsorption on the powdery [60]fullerene surface. This differs from a crystalline [60]fullerene sample, showing an O 1s band found at 533.8 eV attributed to adsorbed water in the X-ray photoelectron spectrum where lower crystallinity causes a significant decrease in the band intensity[16] probably due to a larger surface free energy.[17]

To improve the wettability, we then prepared open-[60]fullerenols, $C_{60}(OH)_2O_3R_2$ (**1**, R_2 = $(CPh)_2NCPy$), $C_{60}(OH)(H)O_3R_2$ (**2**, R_2 = $(CPh)_2NCPy$), and $C_{60}(OH)O_4R_2$ (**3**, R_2 = $(CPh)_2(NH)CPy$),[18] all of which bear an opening with a ring-atom count of 13 (Fig. 1). The latter two were derived from **1** while they accommodate a single water molecule inside (H_2O@**2** and H_2O@**3**) due to the synthetic feature. We also synthesized H_2O@**1** for a reference. The VH IR spectra are shown in Fig. 2 and 3. Contrary to [60]fullerene, **1** showed a significant spectral change attributed to O–H bands (*ca.* 3800–3000 cm^{-1}) with increasing intensity (Fig. 2). In the differential spectra relative to RH = 1%, there seem to be two bands at *ca.* 3800–3500 and 3500–3000 cm^{-1}, which are typical bands of free and aggregated water, respectively.[19] The bending mode at 1613 cm^{-1} conclusively indicates the surface water adsorption. From the simulation (B3LYP-D3/6-31G(d,p)), the bands at 1768 and 1697 cm^{-1} were assigned to the stretching modes of carbonyl groups, **b** and **a**, respectively, where the former exhibited a larger red-shift upon exposure to higher RHs. This is indicative of the water adsorption concomitantly assisted by the carbonyl groups, **a** and **b**, while the latter is much superior. In the differential spectrum, a complex spectral feature was observed at a fingerprint region (< *ca.* 1600 cm^{-1}), which was absent for [60]fullerene. Thus, the two hydroxy groups in **1** are considered to facilitate the water adsorption even at the curved-π surface. The differential spectra of H_2O@**1**, H_2O@**2**, and H_2O@**3** showed a resemblance to that of **1** (Fig. 3). Note that the band of incarcerated H_2O could not be observed under the measured conditions.[20] As opposed to **1** and H_2O@**1**, a larger red-shift was observed for carbonyl band **a** of H_2O@**2** due to the removal of one hydroxy group from H_2O@**1**, whereas water adsorption on H_2O@**3** occurs with significant assistance from carbonyl group(s), **c** and/or **d**. For all open-[60]fullerenols examined, water adsorption/desorption processes were confirmed to be reversible since spectra always came back to the same line at any RH even once RH was increased to *ca.* 90%.

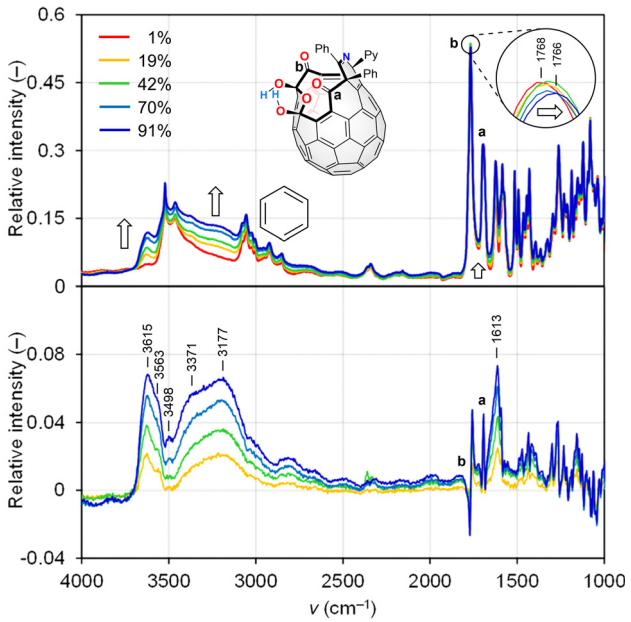

Fig. 2 Original and differential (*vs.* RH = 1%) IR spectra of **1** at 300 K.

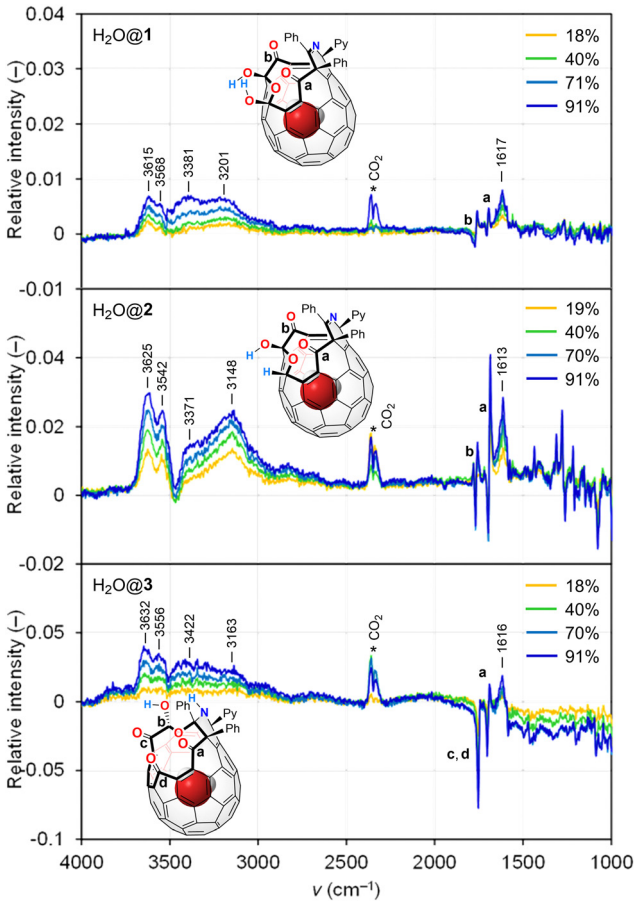

Fig. 3 Differential IR spectra (*vs.* RH = 1%) of H_2O@**1**, H_2O@**2**, and H_2O@**3** at 300 K.

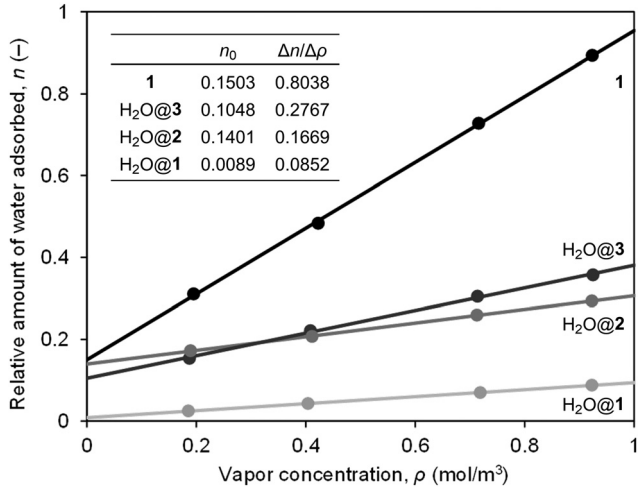

	n_0	$\Delta n/\Delta\rho$
1	0.1503	0.8038
H₂O@**3**	0.1048	0.2767
H₂O@**2**	0.1401	0.1669
H₂O@**1**	0.0089	0.0852

Fig. 4 Relative amounts of water adsorbed on open-[60]fullerenols at variable humidity. The relative amounts were estimated from areas integrated at 3800–2200 cm^{-1} (differential spectra), which were calibrated by the band areas of CH vibrations at 3200–2500 cm^{-1} (original spectra).

From the area ratio for the OH bands in the differential spectra, relative amounts of water adsorbed were estimated, giving a linear relationship with vapor concentrations in air (Fig. 4). It should be noted that all fitted lines did not pass through the origin, implying the presence of water adsorbed even under dry conditions, whose amounts follow the order of H₂O@**2** > H₂O@**3** > H₂O@**1**. From the slope, affinity to water was found to follow the order of H₂O@**3** > H₂O@**2** > H₂O@**1** even though **1** bears two hydroxy groups on its orifice. The replacement of one of the hydroxy groups with a hydrogen atom (H₂O@**1** to H₂O@**2**) was suggested to induce a local positive potential area on the [60]fullerene cage while the whole caged surface of H₂O@**3** is positively charged due to the electron-withdrawing character of the three carbonyl groups (Fig. 5a). Thus, the Lewis acidity of carbon cages[21] is considered to play a significant role in water affinity while OH and/or NH groups should be a trigger to initiate water adsorption.

To our surprise, placing a water molecule inside **1** considerably decreases water affinity by one tenth (Fig. 4). To clarify the origin of the change in adsorptive character, we performed topological analysis (Fig. 5b), showing weak non-covalent interactions between incarcerated H₂O and the hemispherical caged surface where H₂O and O(3) were connected *via* a bond path characterized by a bond critical point (BCP) with positive Laplacian ($\nabla^2\rho$ = 3.46 × 10^{-2} *e* a_0^{-5}) and total energy (H = 8.19 × 10^{-5} a.u. a_0^{-3}) of electron density. Thus, H₂O@**1** is considered to possess an intramolecular H-bonding which is categorized as a pure closed-shell interaction without covalent nature.[22] The interaction energy was estimated to be $E^{(2)}$ 2.56 kcal mol^{-1} (n(O(3)) → σ^*(H₂O)). Upon encapsulation of H₂O, **1** receives a small distortion (ΔG + 0.365 kcal mol^{-1}) whose geometry itself (**1′**) does not cause a significant change in the electronic properties. However, interaction with water results in an elevated LUMO level by net +0.031 eV, indicating the reduced Lewis acidity which contributes to lower $\Delta n/\Delta\rho$ relative to pristine **1**. In addition, the polarization of the two hydroxy groups is suggested to become weaker with smaller Δq values. This might be attributed to the diminished amount of water adsorbed under dry conditions (smaller n_0).

The band deconvolution analysis of **1** at RH = 91% showed the presence of multiple bands (Fig. 6) where **A** and **B** are free water probably spread over the [60]fullerene surface while **D** and **E** originate from distorted and non-distorted ice-like water networks structured by the two hydroxy groups.[19] Though band **C** is not usually observed for bulk water, it likely arises from unstable/short-lived small water clusters aggregated on the π-surface *via* defective H-bondings. Importantly, we also found multiple bands below 3000 cm^{-1} (**F–I**) which cover 14.1% of the whole OH spectral bands (3750–2410 cm^{-1}). These are typical of flanking water around protons (2500 ± 500 cm^{-1}).[23] To our surprise, gas-phase acidity values[24] of the two hydroxy groups in **1** were calculated to be ΔH 334 and 335 kcal mol^{-1} (B3LYP-D3/6-31G(d,p)) which were far smaller than those for PhOH (361 kcal mol^{-1}) and *t*-BuOH (392 kcal mol^{-1}) but rather similar to those for HCl (343 kcal mol^{-1}) and HBr (328 kcal mol^{-1}), indicating that open-[60]fullerenols are highly acidic (Fig. 6b and Fig. S7, ESI†). This rationally explains the presence of bands, **F–I**. Thereby, open-[60]fullerenols are considered to enhance the local acidity of water adsorbed owing to their high electron-accepting character. The significantly red-shifted band (ν 2855 cm^{-1}) of adsorbed water with an elongated

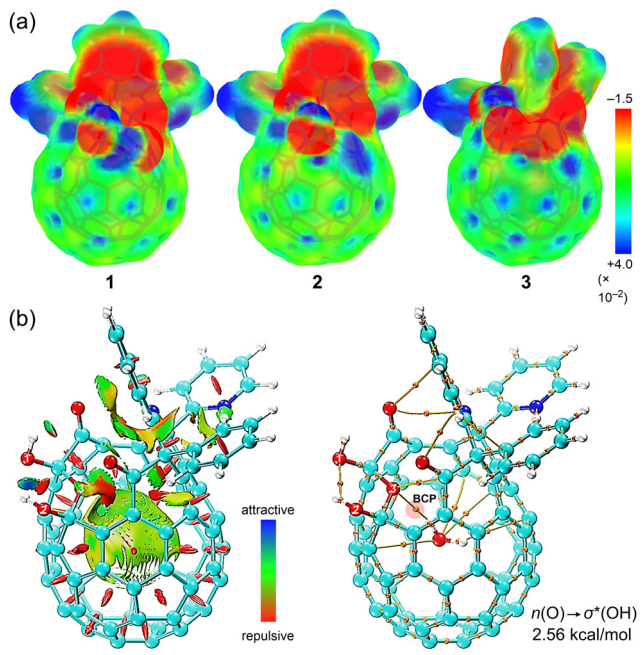

Compd.	LUMO	$q_{O(1)}$	$q_{H(1)}$	Δq_1	$q_{O(2)}$	$q_{H(2)}$	Δq_2
1	–3.170	–0.7544	+0.5103	+1.2647	–0.7342	+0.5038	+1.2380
H₂O@**1**	–3.134	–0.7520	+0.5115	+1.2635	–0.7313	+0.5051	+1.2364
1'	–3.165	–0.7539	+0.5113	+1.2651	–0.7328	+0.5046	+1.2374

Fig. 5 (a) Electrostatic potential maps of **1–3** and (b) topological analysis of electron densities for H₂O@**1** with selected natural charges (units in au) and LUMO levels (units in eV) (B3LYP-D3/6-31G(d,p)). The geometry of **1′** is generated by subtracting a coordinate of H₂O from that of H₂O@**1**.

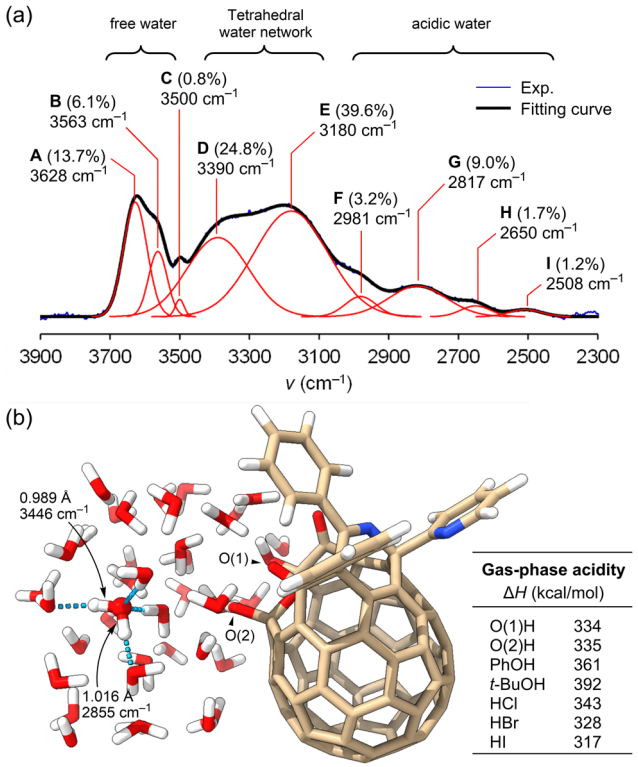

Fig. 6 (a) Band deconvolution analysis of **1** at RH = 91%. (b) Local minimum structure of 1·$(H_2O)_{39}$ with gas-phase acidity for selected alcohols and hydrogen halides (B3LYP-D3/6-31G(d,p) and LanL2DZ for halogen).

OH bond (1.016 Å) was also supported by theoretical calculations for a local minimum structure of **1**·$(H_2O)_{39}$ (Fig. 6b and Fig. S8–S10, ESI†).

In summary, we examined the adsorptive behaviour of water onto the [60]fullerene surface using synchrotron IR microspectroscopy, showing reversible water adsorption/desorption. The VH IR measurements revealed the presence of water adsorbed on open-[60]fullerenols even under dry conditions while the water affinity is governed by the surface electrostatic potential. To our surprise, molecular water adsorption from the internal sphere resulted in a considerable drop of the water affinity at the external sphere mainly because of lowering the Lewis acidity of the [60]fullerene cage while a high electron-accepting character of [60]fullerenols increases the local acidity of water adsorbed.

Financial support was partially provided by the JSPS KAKENHI Grant Numbers JP23H01784, JP23K17916, JP22H04538, and JP19H05717, The Mazda Foundation, and Advanced Technology Institute Research Grants 2023. IR measurements were carried out at SPring-8 (BL43IR) with the approval of JASRI (2021B1298, 2022A1285, and 2022B1138).

Conflicts of interest

There are no conflicts to declare.

Notes and references

1 R. Garcia, *ACS Nano*, 2023, **17**, 51–69.
2 A. Alexiadis and S. Kassinos, *Chem. Rev.*, 2008, **108**, 5014–5034.
3 (*a*) L. Shi and L. Gan, *J. Phys. Org. Chem.*, 2013, **26**, 766–772; (*b*) Y. Hashikawa and Y. Murata, *Bull. Chem. Soc. Jpn.*, 2023, **96**, 943–967.
4 A. L. Smith, M. V. Korobov, A. L. Mirakyan, N. V. Avramenko and E. B. Stukalin, *J. Phys. Chem. B*, 2001, **105**, 2499–2506.
5 R. Rivelino and F. D. B. Mota, *Nano Lett.*, 2007, **7**, 1526–1531.
6 P. Scharff, K. Risch, L. Carta-Abelmann, I. M. Dmytruk, M. M. Bilyi, O. A. Golub, A. V. Khavryuchenko, E. V. Buzaneva, V. L. Aksenov, M. V. Avdeev, Y. I. Prylutskyy and S. S. Durov, *Carbon*, 2004, **42**, 1203–1206.
7 L. Li, D. Bedrov and G. D. Smith, *J. Chem. Phys.*, 2005, **123**, 204504.
8 S. R. Varanasl, O. A. Guskova, A. John and J.-U. Sommer, *J. Chem. Phys.*, 2015, **142**, 224308.
9 H. Wu, L. Lin, P. Wang, S. Jiang, Z. Dai and X. Zou, *Chem. Commun.*, 2011, **47**, 10659–10661.
10 K. Harano and E. Nakamura, *Acc. Chem. Res.*, 2019, **52**, 2090–2100.
11 P. Ravat, H. Uchida, R. Sekine, K. Kamei, A. Yamamoto, O. Konovalov, M. Tanaka, T. Yamada, K. Harano and E. Nakamura, *Adv. Mater.*, 2022, **34**, 2106465.
12 R. Kumar, P. Kumar, S. Naqvi, N. Gupta, N. Saxena, J. Gaur, J. K. Maurya and S. Chand, *New J. Chem.*, 2014, **38**, 4922–4930.
13 T. H. Goswami, B. Nandan, S. Alam and G. N. Mathur, *Polymer*, 2003, **44**, 3209–3214.
14 A. Dawid, K. Górny and Z. Gburski, *J. Phys. Chem. C*, 2017, **121**, 2303–2315.
15 H. Yamagishi, S. Nakajima, J. Yoo, M. Okazaki, Y. Takeda, S. Minakata, K. Albreht, K. Yamamoto, I. Badia-Daminguez, M. M. Oliva, M. C. R. Delgado, Y. Ikemoto, H. Sato, K. Imoto, K. Nakagawa, H. Tokoro, S.-I. Ohkoshi and Y. Yamamoto, *Commun. Chem.*, 2020, **3**, 118.
16 D. Erbahar, T. Susi, X. Rocquefelte, C. Bittencourt, M. Scardamaglia, P. Blaha, P. Guttmann, G. Rotas, N. Tagmatarchis, X. Zhu, A. P. Hitchcock and C. P. Ewels, *Sci. Rep.*, 2016, **6**, 35605.
17 (*a*) Y. Tajima, T. Matsuura, Y. Numata, D. Yamazaki, H. Kawamura and H. Osedo, *Jpn. J. Appl. Phys.*, 2008, **47**, 5730; (*b*) X. Ma, B. Wigington and D. Bouchard, *Langmuir*, 2010, **26**, 11886–11893.
18 (*a*) Y. Hashikawa, K. Kizaki, T. Hirose and Y. Murata, *RSC Adv.*, 2020, **10**, 40406–40410; (*b*) Y. Hashikawa, S. Hasegawa and Y. Murata, *Org. Lett.*, 2021, **23**, 3854–3858; (*c*) Y. Hashikawa, K. Kizaki and Y. Murata, *Chem. Commun.*, 2021, **57**, 5322–5325.
19 M. Śmiechowski and J. Stangret, *J. Mol. Struct.*, 2008, **878**, 104–115.
20 A. Shugai, U. Nagel, Y. Murata, Y. Li, S. Mamone, A. Krachmalnicoff, S. Alom, R. J. Whitby, M. H. Levitt and T. Rõõm, *J. Chem. Phys.*, 2021, **154**, 124311.
21 J. Iglesias-Sigüenza and M. Alcarazo, *Angew. Chem., Int. Ed.*, 2012, **51**, 1523–1524.
22 (*a*) W. Nakanishi, S. Hayashi and K. Narahara, *J. Phys. Chem. A*, 2009, **113**, 10050–10057; (*b*) Y. Hashikawa and Y. Murata, *J. Am. Chem. Soc.*, 2019, **141**, 12928–12938.
23 (*a*) M. Thämer, L. D. Marco, K. Ramasesha, A. Mandal and A. Tokmakoff, *Science*, 2015, **350**, 78–82; (*b*) N. Agmon, *Nat. Chem.*, 2016, **8**, 206–207; (*c*) C. A. Daly Jr, L. M. Streacker, Y. Sun, S. R. Pattenaude, A. A. Hassanali, P. B. Petersen, S. A. Corcelli and D. Ben-Amotz, *J. Phys. Chem. Lett.*, 2017, **8**, 5246–5252; (*d*) J. A. Fournier, W. B. Carpenter, N. H. C. Lewis and A. Tokmakoff, *Nat. Chem.*, 2018, **10**, 932–937.
24 J. E. Bartmess, J. A. Scott and R. T. Mclver Jr, *J. Am. Chem. Soc.*, 1979, **101**, 6046–6056.

